Properties of the fractal measure describing the hydrodynamic force distributions for fractal aggregates moving in a quiescent fluid

Paul Meakin
Central Research and Development Department, Experimental Station, E. I. du Pont de Nemours and Company, Wilmington, Delaware 19898

John M. Deutch
Department of Chemistry, Massachusetts Institute of Technology, Cambridge, Massachusetts 02139

(Received 3 December 1986; accepted 6 January 1987)

Using the Kirkwood–Riseman theory we show that the penetration of the hydrodynamic field for a fractal aggregate (diffusion-limited cluster–cluster aggregate) moving with a constant translational velocity with respect to a fluid can be described in terms of a fractal measure. The spectrum of singularities, $f(\alpha)$ of strength α defined by Halsey *et al.* has been estimated by scaling the total force distribution and the distribution of force components parallel and perpendicular to the relative velocity for aggregates of different sizes. The scaling of the moments of the force and force component distributions with the cluster mass has also been investigated. Each moment scales with a different exponent which is related to the spectrum $f(\alpha)$ and the corresponding infinite hierarchy of fractal dimensionalities D_q.

INTRODUCTION

In recent years considerable interest has developed in nonequilibrium growth and aggregation processes which frequently lead to the formation of fractal structures.[1] Much of this interest has been focused on the Witten–Sander[2] model for diffusion-limited aggregation in which particles are added, one at a time, to a growing cluster or aggregate of particles via random walk trajectories. This model generates clusters with a fractal geometry (which is still not yet fully understood) and has directly or indirectly stimulated much of the recent work on fractal aggregates. The Witten–Sander model provides a basis for understanding a wide variety of important processes but not colloidal aggregation. A more realistic representation of colloidal aggregation is provided by the diffusion-limited cluster–cluster aggregation model[3,4] and related cluster–cluster aggregation models.[5] In particular, the diffusion-limited cluster–cluster aggregation model leads to results for both the structure and dynamics of the aggregation of small metal particles under fast aggregation conditions which are in good agreement with experimental results.[6,7] For most models and experimental systems, interest was first focused on characterizing the fractal geometry. At a later stage considerable effort was devoted to the kinetics of growth or aggregation[8] and the physical properties of fractals[9–11] including their translational friction coefficients[12,13] (obtained from the total force on a cluster moving with a constant velocity).

It has been known for some time that for systems with a fractal measure an infinite hierarchy of moments and associated fractal dimensionalities are needed to describe their structure.[14–17] The earliest examples were associated with dynamic systems such as turbulence in fluids[14] and strange attractors.[16] More recently, it has been found that fractal measures can be used to describe a broader range of physical processes such as the growth of fractal aggregates,[18–23] the penetration of particles and fields into a variety of fractal structures, and the voltage distribution in conducting percolation clusters.[24,25] Recently, Halsey *et al.*[26] and Kadanoff[27] have proposed a general picture for fractal measures in terms of a continuous spectrum, $f(\alpha)$ of singularities of type or strength α. According to this picture the quantity $f(\alpha)$ is the fractal dimensionality of the subset on which the singularities of strength α lie. The infinite hierarchy of fractal dimensionalities (D_q^{16}) and exponents γ_n^{20} describing the scaling properties of the moments of the measure are then determined by the shape of the function $f(\alpha)$. Halsey *et al.*[26] show how the quantities D_q and $f(\alpha)$ are related and show how these quantities can be measured. A convenient procedure for obtaining the quantity $f(\alpha)$ by scaling the probability distributions defining the fractal measure for systems of different sizes onto a common curve has been illustrated by Meakin[19] for the growth probability measure (and other fractal measures[28]) on fractal aggregates.

For the case of an aggregate of particles moving through a fluid, the distribution of forces exerted by the fluid on each of the particles can be described in terms of a measure (which we will call the force distribution measure). Since (relatively) large forces will be exerted on the most exposed particles in the outer regions of the cluster and small forces will be exerted from the more deeply buried particles which are screened from the hydrodynamic field, a very broad distribution of forces can be anticipated. It is also reasonable to expect (by analogy with the penetration of a harmonic field into a fractal structure[29,30]) that the measure (force distribution measure) describing the penetration of a hydrodynamic field into a fractal structure will be a fractal measure which can be described in terms of the α, $f(\alpha)$ picture of Halsey *et al.*[26] The main purpose of the work described in this paper was to test this idea. Our main conclusion is that the force distribution measure obtained for three-dimensional diffusion-limited cluster–cluster aggregates with a fractal dimensionality of 1.75–1.8 is a fractal measure which can be described in terms of the α, $f(\alpha)$ picture of Halsey *et al.* Consequently, we find that the α, $f(\alpha)$ picture can be used

 0021-9606/87/084648-09$02.10

to describe the penetration of vector as well as scalar fields into fractal structures.

SIMULATIONS AND CALCULATIONS

Three-dimensional aggregates were simulated using an off-lattice version of the diffusion-limited cluster–cluster aggregation model in the zero concentration limit with a constant reaction kernel. This model, which has been described previously,[31,32] generates clusters with a fractal dimensionality of about 1.78. Clusters containing 50, 100, 200, or 400 identical spherical particles were generated starting with a list of particles. To calculate the distribution of hydrodynamic forces we used the same methods which were used earlier[13] to calculate the translational friction coefficient.

Within the framework of the Kirkwood–Riseman[33] theory the force had $\mathbf{F}_i$ exerted by the ith particles on the fluid is given by

$$\mathbf{F}_i + \zeta_0 \sum_{\substack{j=1 \\ (j\neq i)}}^{M} \mathbf{T}_{ij}\cdot\mathbf{F}_j = \zeta_0 \mathbf{U}_i. \tag{1}$$

Here S_0 is the friction coefficient for each of the particles of radius a given by

$$\zeta_0 = 6\pi\eta_0 a, \tag{2}$$

where η_0 is the fluid viscosity. In Eq. (1) $\mathbf{U}_i$ ($\mathbf{U}_i = \mathbf{V}$) is the unperturbed fluid velocity at the ith particle and $\mathbf{T}$ is the hydrodynamic interaction tensor. In this and earlier work[12,13] we have used the modified version of the Oseen[34] tensor introduced by Rotne and Prager[35] and Yamakawa,[36]

$$\mathbf{T}_{ij} = (8\pi\eta_0 r_{ij})^{-1}\left\{\left[\mathbf{I} + (\mathbf{r}_{ij}\mathbf{r}_{ij}/r_{ij}^2)\right] + \frac{2a^2}{r_{ij}^2}\left[\mathbf{I}/3 - (\mathbf{r}_{ij}\mathbf{r}_{ij}/r_{ij}^2)\right]\right\}, \tag{3}$$

where $\mathbf{r}_{ij}$ is the vector from the ith to the jth particles and r_{ij} is the magnitude of this vector. The matrix equation (1) was solved for the forces $\mathbf{F}_i$ using the numerical method described by McCammon and Deutch.[37] The forces $\mathbf{F}_i$ were determined for a uniform velocity ($\mathbf{U}_i = \mathbf{V}$) in three mutually perpendicular but otherwise arbitrary directions (x, y, and z) for each cluster. In this manner the distribution of forces was obtained for 10 000 clusters of 50-particle clusters, 4563 clusters of 100 particles, 749 clusters of 200 particles, and 232 clusters of 400 particles. For each particle in every cluster the components of the force $\mathbf{F}_i$ parallel and perpendicular to the velocity $\mathbf{V}$ and the magnitude of the force were determined.

RESULTS

Figure 1(a) shows the distribution of the force components in a direction parallel to the velocity vector $\mathbf{V}$. Here $F_\parallel$ is the magnitude of the force component in the direction of $\mathbf{V}$ and $N[\ln(F_\parallel)]$ is the number of particles per unit interval of $\ln(F_\parallel)$ with a parallel force component of $F_\parallel$ {i.e., $N[\ln(F_\parallel)]\delta\ln(F_\parallel)$ is the number of particles with parallel force components whose natural logarithm lies in the range $\ln(F_\parallel) \pm \delta\ln(F_\parallel)/2$}. In practice the $\ln(F_\parallel)$ scale is divided into intervals of width 0.1 and the results shown for $N[\ln(F_\parallel)]$ in Fig. 1(a) is a "histogram" showing $10\times$ the average number of particles in each interval [i.e., the number of particles per unit interval of $\ln(F_\parallel)$].

The first step towards obtaining the function $f(\alpha)$ is to obtain a similar histogram for the normalized force distribution[19] defined by

$$(F_\parallel^n)_i = (F)_i / \sum_{j=1}^{M} (F_\parallel)_j. \tag{4}$$

Here $(F_\parallel^n)_i$ is the normalized parallel force component for the ith particle and $(F_\parallel)_i$ is the corresponding unnormalized force component. The logarithmic distribution function for the normalized parallel force components is shown in Fig. 1(b). The curves shown in Figs. 1(a) and 1(b) seem to have a skewed Gaussian shape corresponding to a skewed log-normal distribution of parallel force components. Such "log-normal" distributions are characteristic of fractal measures.

Figure 2 shows the dependence of $\ln(N[\ln(F_\parallel^n)])$ on $\ln(F_\parallel^n)$. It is the scaling of these curves onto a common curve[19] which provides an estimation of the function $f(\alpha)$ of Halsey *et al.*[26] Figure 3 shows the dependence of $\ln(N[\ln(F_\parallel^n)])/\ln(M)$ on $\ln(F_\parallel^n)/\ln(M)$. Plotting the data in this way results in a crude scaling collapse onto a single curve and in the asymptotic limit we expect (for a fractal measure) that

$$\ln(N[\ln(F_\parallel^n)]) = \ln(M)g[\ln(F_\parallel^n)/\ln(M)], \tag{5}$$

where the scaling function $g(x)$ is related to the spectrum of singularities in the measure $[f(\alpha)]$ defined by Halsey *et al.*[26] according to[19]

$$g(x) = D^{-1} f(-Dx) \tag{6a}$$

or

$$f(\alpha) = Dg(-D^{-1}\alpha), \tag{6b}$$

where D is the fractal dimensionality of the cluster.

In view of the rather small cluster sizes used in this work (the hydrodynamic interaction tensor $\mathbf{T}$ has dimensions $3M \times 3M$ which limits the maximum cluster size to about $M = 400$ particles) the scaling collapse onto a single curve shown in Fig. 3 is quite good. Since the fractal dimensionalities for the support of the measure seems to be equal to the fractal dimensionality of the cluster itself, for this problem we expect that the maximum value for the scaling function $g(x)$ should be 1.0. (The subset corresponding to some value of the exponent x or α must grow as rapidly as the cluster mass but no part of the measure can grow faster than the cluster mass.) The maximum value obtained for $g(x)$ (for clusters containing 400 particles) is 0.87. The deviation of this value from 1.0 is attributed to finite size corrections to scaling.

The results shown in Fig. 3 were obtained by normalizing the parallel force components for each cluster moving in each of three mutually perpendicular directions [Eq. (4)]. Almost identical results were obtained by normalizing all of the parallel force components:

$$(F_\parallel^n)_{lmn} = (F_\parallel)_{lmn} / \sum_{i=l}^{M}\sum_{j=l}^{N}\sum_{k=l}^{3} (F_\parallel)_{ijk}, \tag{7}$$

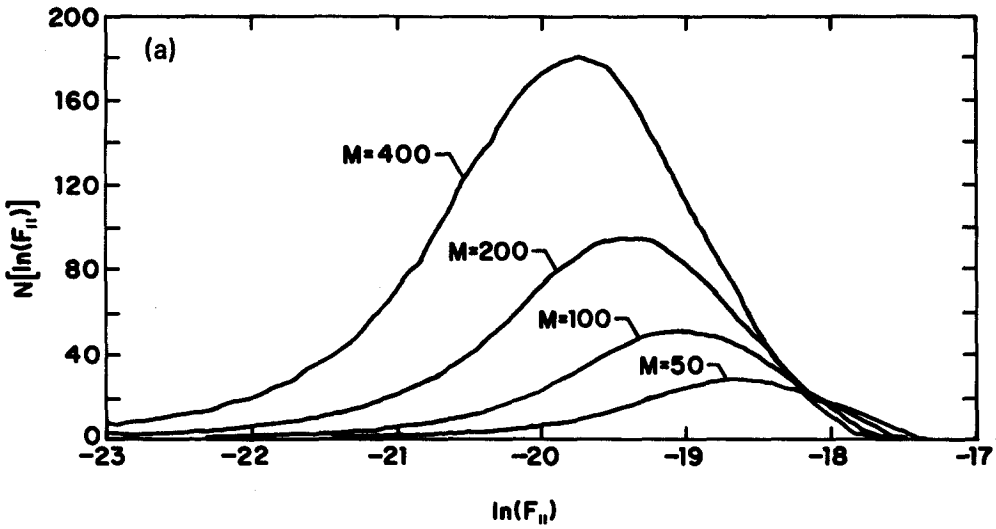

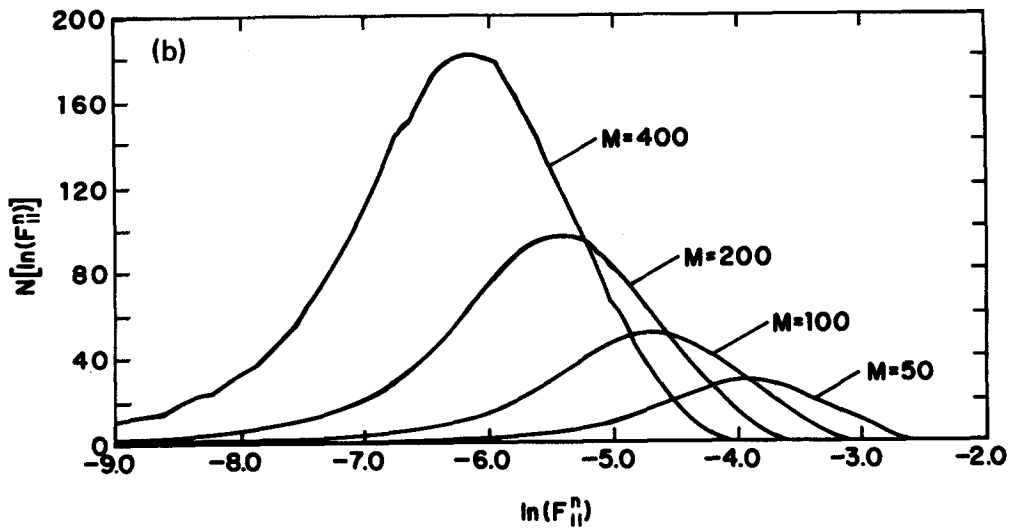

FIG. 1. Logarithmic distributions for the parallel force components for $3d$ cluster–cluster aggregates containing $M = 50$, 100, 200, and 400 particles. Figure 1(a) shows the unnormalized force distributions and Fig. 1(b) shows the forces normalized so that $\Sigma_{i=1}^{M} (F_{\parallel}^{n})_i = 1$.

where $(F_{\parallel})_{ijk}$ is the parallel force component associated with the ith particle in the jth cluster (of size M) moving with fixed orientation in the k th direction with respect to the fluid.

Interpretation of the function $f(\alpha)$ as the fractal dimension of the subset on which singularities of strength α reside suggests that the fractal measure defined by the force distribution should be scaled by plotting $\ln\{N[\ln(F_{\parallel}^{n})]\ln(M)\}/\ln(M)$ vs $\ln(F_{\parallel}^{n})/\ln(M)$.[19] The quantity $N[\ln(F_{\parallel}^{n})]\ln(M)$ is proportional to the number of particles per unit interval associated with a small region on the abscissa in Fig. 3 or a small range in the singularity strength,

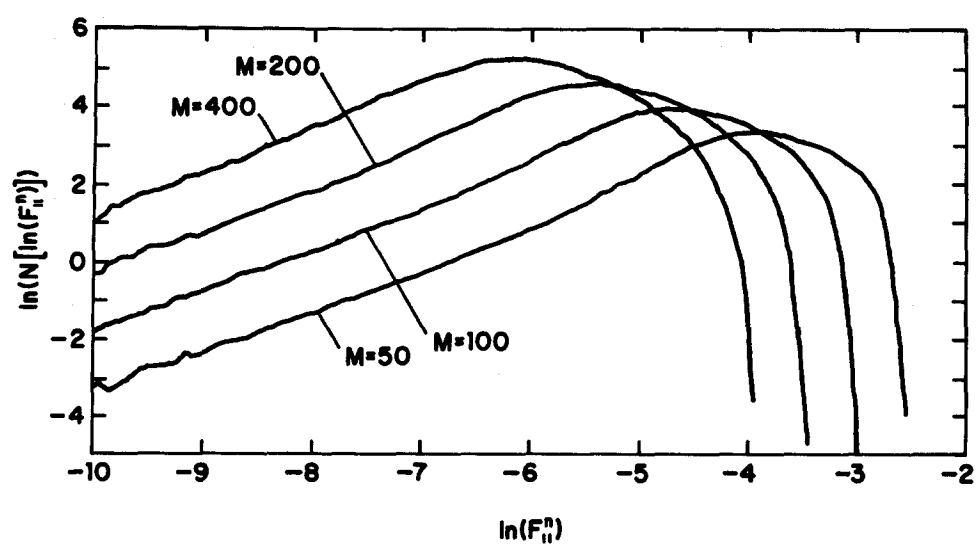

FIG. 2. Dependence of $\ln(N[\ln(F_{\parallel}^{n})])$ on $\ln(F_{\parallel}^{n})$ for $3d$ cluster–cluster aggregates. $F_{\parallel}^{n}$ is the normalized force on the particles in the direction of motion through the fluid.

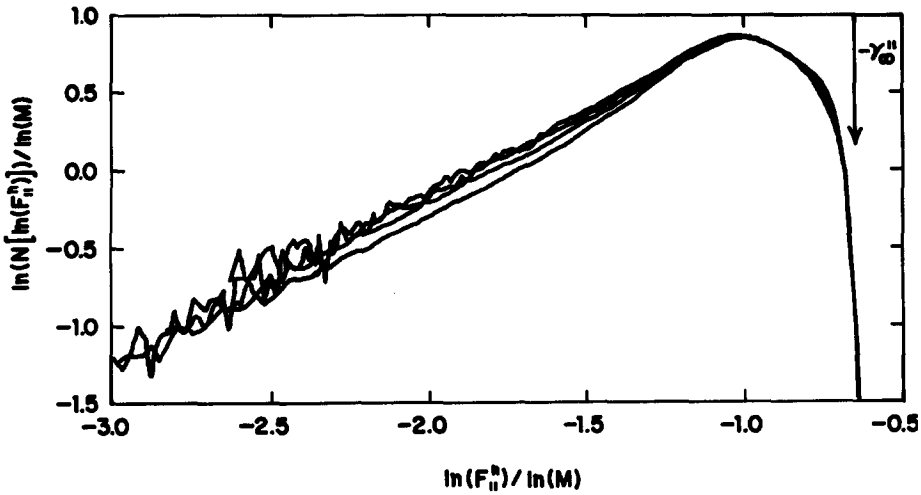

FIG. 3. Scaling of the (logarithmic) force distributions for clusters of different sizes ($M = 50$, 100, 200, and 400 particles) shown in Fig. 2.

α. Figure 4 shows the data collapse obtained in this way. Now the maximum value in the scaling function $g'(x)$, defined by

$$\ln(N[\ln(F_\parallel^n)]\ln(M)) = \ln Mg'[\ln(F_\parallel^n)/\ln(M)], \quad (8)$$

has a value greater than 1.0 but this maximum value decreases with increasing cluster size.

In the limit $M \to \infty$ we expect that $g(x)$ and $g'(x)$ will converge onto the same curve with a maximum value of 1.0. This idea seems to be consistent with our results. Figures 3 and 4 strongly suggest that the distribution of parallel force components can be described in terms of a fractal measure. Data collapse using the scaling forms given in Eqs. (5) and (8) and illustrated in Figs. 3 and 4 are based on the fact that $\ln[Y(x)]/\ln(x) = C$ (where C is a constant) for all values of x if $Y(x) \sim Ax^C$ and the factor A has a value of 1.0. If A has a value other than 1.0 $\ln[Y(x)]/\ln(x)$ will only converge to a value of C as $x \to \infty$. Figure 5 shows the scaling behavior obtained by plotting $\ln(aN[\ln(F_\parallel^n)]\ln(M))/\ln(M)$ against $\ln(F_\parallel^n)/\ln(M)$ with $a = 0.4$. This procedure gives a maximum value for the scaling function close to 1.0 and a good data collapse for forces larger than those corresponding to the maximum value for the scaling function. The scaling function corresponding to this procedure is given by

$$\ln(aN[\ln(F_\parallel^n)]\ln(M)) = \ln(M)g''[\ln(F_\parallel^n)/\ln(M)]. \quad (9)$$

More elaborate attempts to account for corrections to the asymptotic scaling behavior could be envisaged but are not justified by our data.

Very similar results have been obtained for the component of the force perpendicular to the direction of motion of the fluid relative to the cluster. Figure 6 shows the scaling collapse obtained using the most simple of the scaling procedures discussed above [Eq. (5)] for the magnitude of the perpendicular component of the force ($F_\perp$). As for the parallel component, the normalized force distribution ($F_\perp^n$) is used to obtain the scaling function which describes the force distribution measure. Figure 7 shows very similar results obtained for the distribution of the magnitudes of the total forces associated with the particles in cluster–cluster aggregates. Again, the simple scaling form given in Eq. (5) works very well.

For a small fraction of the particles (about 2%) the force exerted by the particle on the fluid has a component which is parallel to but with a direction opposite to the direction of motion of the cluster with respect to the fluid. The distribution of these antiparallel force components (F_-) is

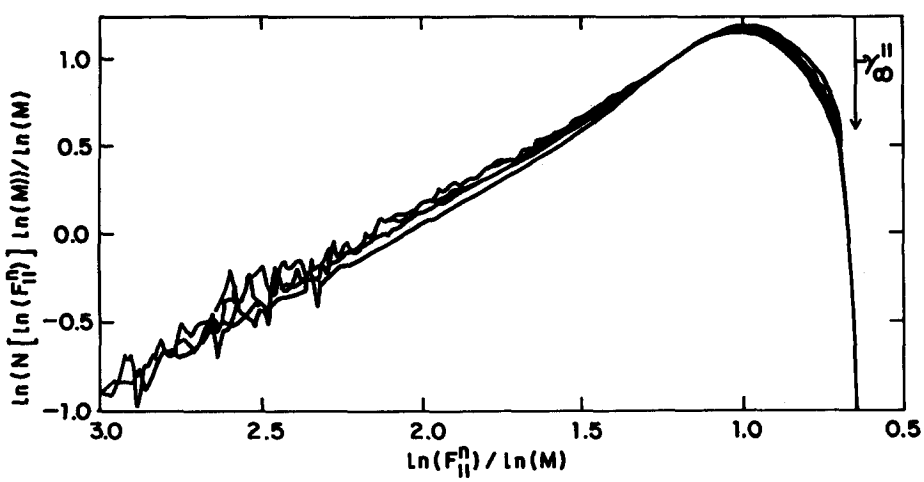

FIG. 4. An alternative procedure for scaling the parallel component force distribution curves shown in Fig. 2. This procedure includes an expected logarithmic correction to scaling which is not included in the scaling procedure used to obtain Fig. 3.

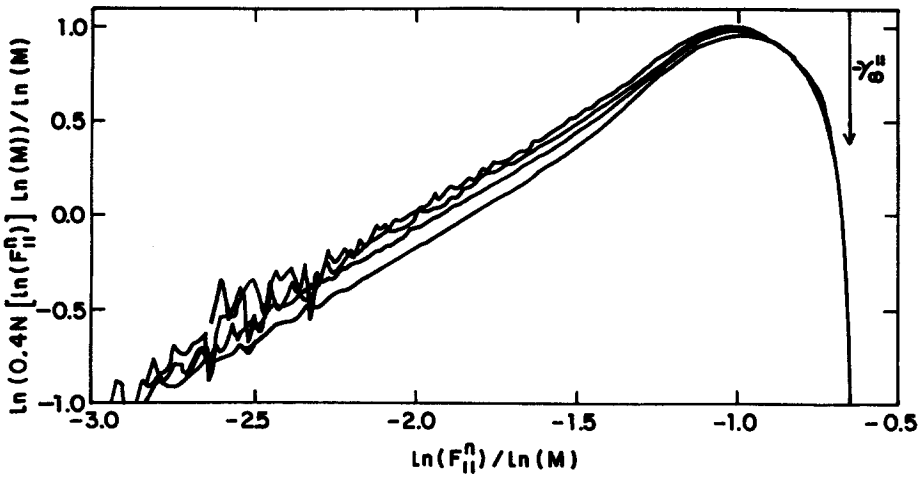

FIG. 5. Scaling of the distribution of parallel force components using the scaling form given in Eq. (8).

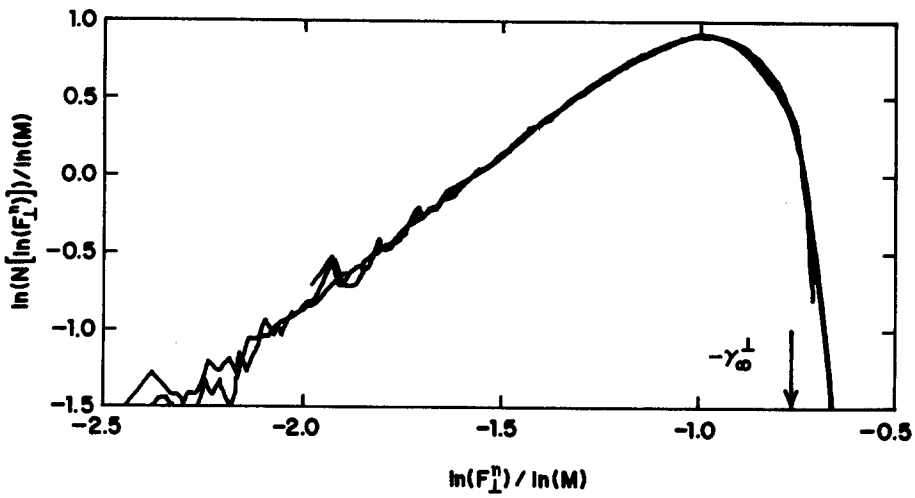

FIG. 6. Scaling of the distribution of the perpendicular components of the forces on particles in clusters containing 50, 100, 200, and 400 particles.

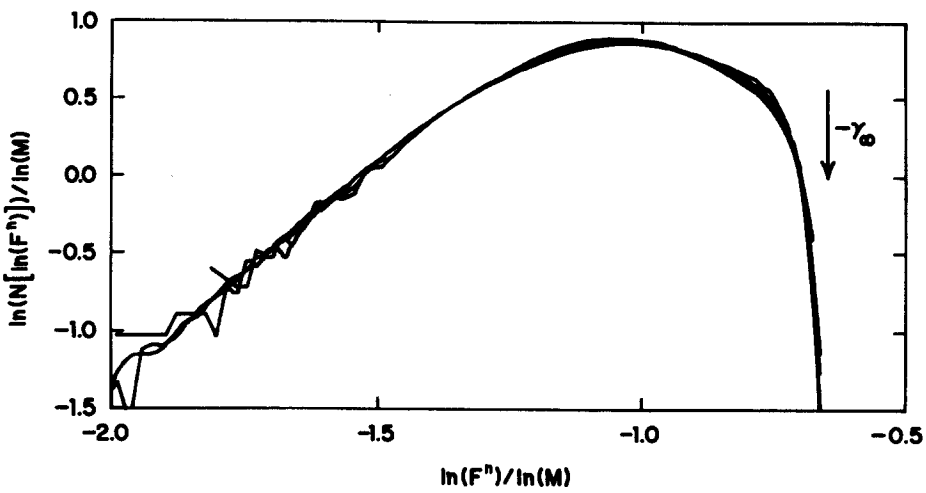

FIG. 7. Scaling of the normalized (logarithmic) distribution of the total force on particles in 3*d* diffusion-limited cluster–cluster aggregates containing 50, 100, 200, and 400 particles. The simple scaling form given in Eq. (5) was used.

shown in Fig. 8. The antiparallel forces were included with the parallel forces in Figs. 1–5. Since only a small fraction of the forces have antiparallel components very similar results would have been obtained if they had been omitted.

MOMENTS OF THE FORCE DISTRIBUTIONS

An important characteristic of a fractal measure is the scaling properties of different moments of the measure. For the force distribution measure we are interested in moments such as[20,21]

$$\mu_n = \left[\frac{1}{\sum_{i=1}^{M} f_i^{n+1}}\right]^{1/n}. \tag{10}$$

Here f_i is the force (or force component) exerted by the ith particle on the fluid. For aggregates of different sizes (M) we expect that the moments μ_j will scale with the cluster mass (M) according to

$$\mu_j \sim M^{-\gamma_j}, \tag{11}$$

where the exponents γ are all different for different values if the forces f_i constitute a fractal measure. In general, j need not be an integer but here we have confined ourselves to the case where j is a small positive integer ($j = 1 - 8$). The exponents γ_j are related to the fractal dimensions D_q defined by Hentschel and Procaccia by

$$D_q|_{q=j+1} = D^{\gamma_j}. \tag{12}$$

Both the dimensionalities D_q and the exponents γ_j can (at least in principle) be obtained from the functions $f(\alpha)$[26] or $g(x)$. However, in practice more reliable results can generally be obtained by a direct measurement of these quantities.

Figures 9(a), 9(b), and 9(c) show the dependence of the moments $\mu_n^{\parallel}$, $\mu_n^{\perp}$, and μ_n [Eq. (10)] obtained from the parallel force components, perpendicular force components, and the total forces, respectively, for $n = 1$–6. Despite the rather small cluster sites the dependence of the natural logarithms of these moments of $\ln(M)$ is surprisingly linear. Table I shows the corresponding exponents ($\gamma_n^{\parallel}$, $\gamma_n^{\perp}$, and γ_n) obtained from least-squares fitting straight lines to the dependence of $\ln(\mu)$ or $\ln(M)$. The standard errors for the exponents are quite small (less than 0.001) in all cases. The dependence of $\gamma_n^{\parallel}$, $\gamma_n^{\perp}$, and γ_n on n is shown in Fig. 10. The results shown in this figure indicate that the limiting (large n) exponents for the maximum force or force components have values of approximately 0.645 for $F_{\parallel}^n(\gamma_{\infty}^{\parallel})$, 0.77 for $F_{\perp}^n(\gamma_{\infty}^{\perp})$, and 0.655 for $F_n(\gamma_{\infty})$. The values of these limiting exponents are indicated by vertical arrows in Figs. 3–7.

DISCUSSION

The results presented above show that the distribution of forces exerted by the particles in a fractal aggregate moving with a constant translational velocity with respect to a quiescent fluid can be described in terms of a fractal measure. Although our results have been obtained using aggregates generated using the diffusion limited cluster–cluster aggregation model assuming a simplified form for the hydrodynamic interaction tensor [Eq. (3)], our qualitative results should be generally true for fractal structures moving in a fluid.

An interesting feature of the scaling functions $[g(x)]$ found in Figs. 3–7 is the existence of regions with negative values for both large and small x. The number of particles corresponding to these parts of the measure is quite small and there is some indication that these negative parts of the effective scaling function do not exist in the limit $M \to \infty$. The negative parts of $g(x)$ may correspond to particles with forces smaller than or larger than the ensemble average minimum and maximum values, respectively.[38]

Another significant feature of the scaling functions shown in Figs. 3–7 is the apparent existence of a maximum value for the derivative $d[g(x)]/dx$. The exponent γ_n is determined by the value of x for which $d[g(x)]/dx = -(n+1)$,[26]

$$\left.\frac{dg(x)}{dx}\right|_{x=x(n)} = -(n+1) \tag{13}$$

and the exponent γ_n is given by

$$\gamma_n = -1/n\{(n+1)x(n) + g[x(n)]\}. \tag{14}$$

If the scaling function $g(x)$ has a constant slope for large negative values of x,

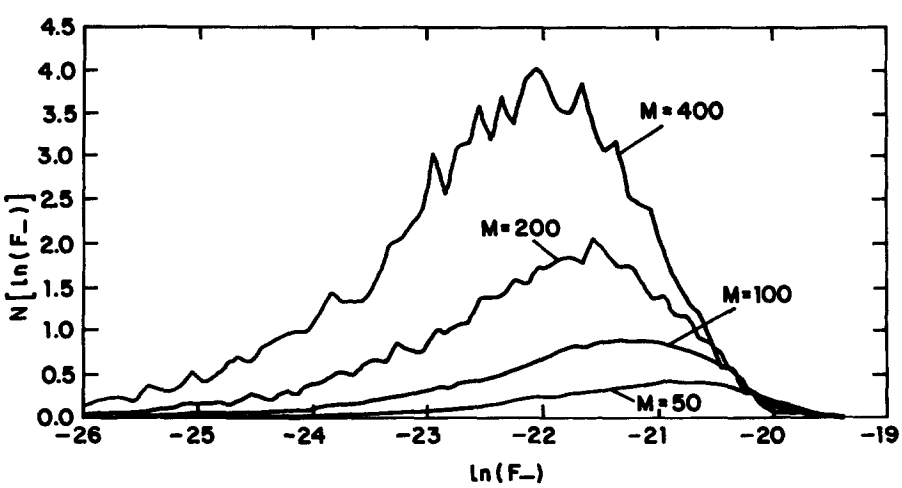

FIG. 8. Logarithmic distribution for the antiparallel components of the force distribution for 3d cluster–cluster aggregates. This figure should be compared with Fig. 1.

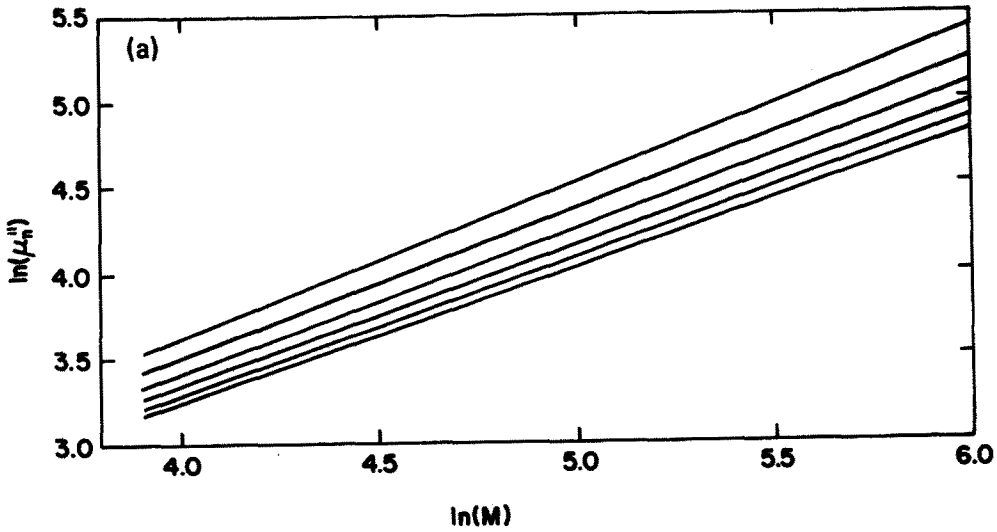

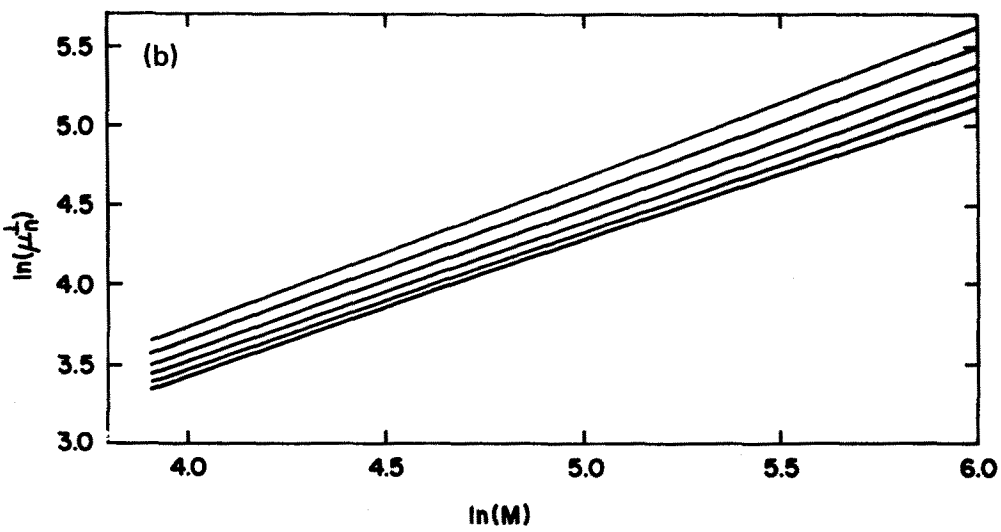

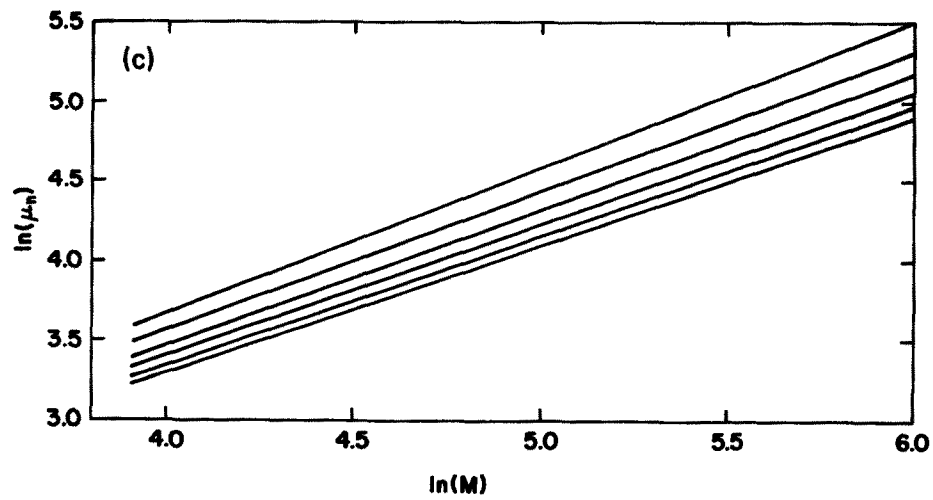

FIG. 9. Dependence of the moments $\mu_n^{\parallel}$, $\mu_n^{\perp}$, and μ_n on the cluster mass (M) for clusters containing 50, 100, 200, and 400 particles. Results for $n = 1$–6 are shown in this figure. Figure 9(a) shows the moments $\mu_n^{\parallel}$ obtained from the parallel force components. Figure 9(b) shows the moments of the perpendicular force components Fig. 9(c) shows the moments of the total force components. The largest values of n correspond to the lowest curves with the smallest slopes.

TABLE I. Values for the exponents $\gamma_n^{\parallel}$, $\gamma_n^{\perp}$, and γ_n obtained from the corresponding force distribution moments $\mu_n^{\parallel}$, $\mu_n^{\perp}$, and μ_n for $n = 1$–8. The standard errors for the linear least-square fits used to obtain the exponents are less than 0.001 in all cases. Systematic errors are almost certainly larger. Some selected exponents for higher values of n are also given.

	Exponents		
n	$\gamma_n^{\parallel}$	$\gamma_n^{\perp}$	γ_n
1	0.899	0.940	0.912
2	0.862	0.914	0.876
3	0.834	0.891	0.849
4	0.812	0.872	0.827
5	0.795	0.856	0.810
6	0.781	0.844	0.796
7	0.769	0.833	0.785
8	0.759	0.825	0.775
10	0.747	0.816	0.759
15	0.722	0.797	0.734
20	0.704	0.788	0.723
30	0.689	0.780	0.704
40	0.679	0.777	0.694
60	0.669	0.777	0.684
80	0.665	···	0.680

$$\frac{dg(x)}{dx} \leqslant c, \tag{15}$$

all moments μ_n for $n < -(c+1)$ will diverge. If, on the other hand, the curves $g(x)$ terminate at the point (x_0) where the effective scaling functions intersect the abscissa then $x(n) = x_0$ for $n < -(c+1)$ and γ_n will be given by

$$\gamma_n = -1/n[(n+1)x_0] \tag{16}$$

for large negative values of n (the large negative moments will be determined by singularities of strength $-Dx_0$ and there will be a constant "gap" x_0 for the exponents γ_n corresponding to these moments). Similarly, if the scaling function $g(x)$ terminates with a finite slope at the point $x = x_0'$ on the abscissa for the largest values of x then the moment μ_n with large n will scale with the mass with exponents which also exhibit a constant gap (all of the high moments will be determined by singularities of strength $-Dx_0'$).

Figure 10(b) shows the dependence of $(n/n+1)\gamma$ (for $\gamma_n^{\parallel}$, $\gamma_n^{\perp}$, and γ_n with n in the range 1–80) on $1/n$. For the case of a constant gap and $g[x(n)] = 0$ for large n we would expect $(n/n+1)\gamma$ to be independent of n for large n (small

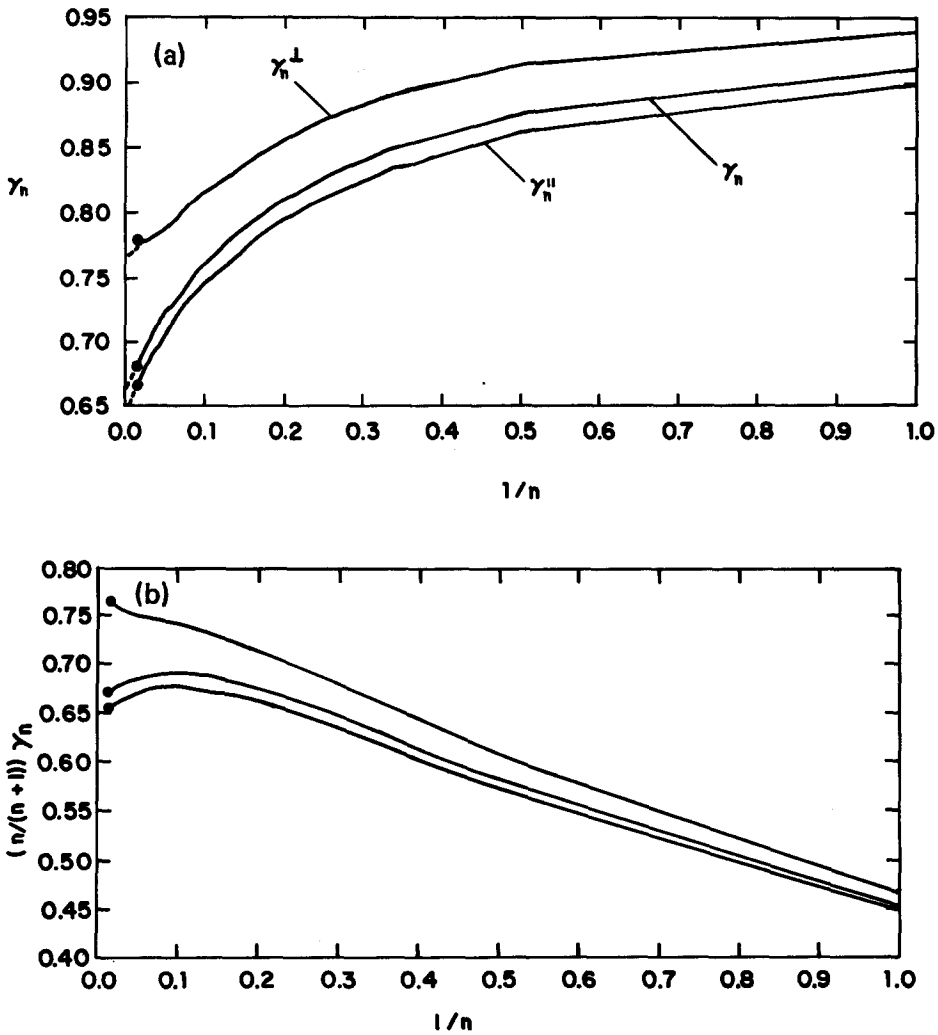

FIG. 10. Dependence of the exponents $\gamma_n^{\parallel}$, $\gamma_n^{\perp}$, and γ_n on n for values of n up to 80. Figure 10(a) shows the dependence of γ on $1/n$ and Fig. 10(b) shows the dependence of $(n/n+1)\gamma$ on $1/n$. The large solid dots indicate the coordinates (n,γ_n) for the larger values of n.

$1/n$). The results shown in this figure are not conclusive.

The broad distribution of forces which generate the fractal measures are a result of the strong screening of the hydrodynamic field from penetration into the cluster. The total force exerted by the fluid on the cluster is concentrated into the most peripheral particles. This may have important implications for the mechanical stability of large aggregates moving through a fluid.[39]

ACKNOWLEDGMENT

We would like to thank T. A. Witten for suggesting this work and for helpful discussions.

[1]B. B. Mandelbrot, *The Fractal Geometry of Nature* (Freeman, San Francisco, 1982).
[2]T. A. Witten and L. M. Sander, Phys. Rev. Lett. **47**, 1400 (1981).
[3]P. Meakin, Phys. Rev. Lett. **51**, 1119 (1983).
[4]M. Kolb, R. Botet, and R. Jullien, Phys. Rev. Lett. **51**, 1123 (1983).
[5]R. Jullien, R. Botet, and M. Kolb, La Recherche **171**, 1334 (1985).
[6]S. R. Forrest and T. A. Witten, J. Phys. A **12**, L109 (1979).
[7]D. A. Weitz and M. Oliveria, Phys. Rev. Lett. **52**, 1433 (1984).
[8]F. Family, P. Meakin, and T. Vicsek, Rev. Mod. Phys. (to be published).
[9]In *Proceedings of the Sixth Trieste International Symposium on Fractals in Physics*, edited by L. Pietronero and E. Tosatti (North-Holland, Amsterdam, 1986).
[10]*On Growth and Form: Fractal and Nonfractal Patterns in Physics*, NATO ASI Series E100, edited by H. E. Stanley and N. Ostrowky (Martinus Nijhoff, Dordrecht, 1986).
[11]H. J. Hermann, Phys. Rep. **136**, 153 (1986).
[12]Z. Y. Chen, J. M. Deutch, and P. Meakin, J. Chem. Phys. **80**, 2082 (1984).
[13]P. Meakin, Z. Y. Chen, and J. M. Deutch, J. Chem. Phys. **82**, 3786 (1985).
[14]B. B. Mandelbrot, J. Fluid Mech. **62**, 331 (1974).
[15]B. B. Mandelbrot, Ann. Isr. Phys. Soc. **2**, 226 (1978).
[16]H. G. E. Hentschel and I. Procaccia, Physica D **8**, 435 (1983).
[17]B. B. Mandelbrot, *Proceedings of the International Workshop on Dimensions and Entropies in Chaotic Systems, Pecos River, New Mexico, 1985*, edited by G. Meyer-Kress (Springer, Berlin, 1986).
[18]T. C. Halsey, P. Meakin, and I. Procaccia, Phys. Rev. Lett. **56**, 854 (1986).
[19]P. Meakin, Phys. Rev. A **34**, 710 (1986).
[20]P. Meakin, H. E. Stanley, A. Coniglio, and T. A. Witten, Phys. Rev. A **32**, 2364 (1985).
[21]P. Meakin, A. Coniglio, H. E. Stanley, and T. A. Witten, Phys. Rev. A **34**, 3325 (1986).
[22]C. Amitrano, A. Coniglio, and F. di Liberto, Phys. Rev. Lett. **57**, 1016 (1986).
[23]L. Pietronero, C. Evenqsz, and A. P. Siebesma, in *Stochastic Processes in Physics and Engineering*, edited by S. Albeverio, P. L. Blanchard, L. Streit, and M. Hazelwinkel (Reidel, Dordrecht, 1986).
[24]L. DeArchangelis, S. Redner, and A. Coniglio, Phys. Rev. B **31**, 4725 (1985).
[25]R. Blumenfeld, Y. Meir, A. Brooks Harris, and A. Aharony (preprint).
[26]T. C. Halsey, M. H. Jensen, L. P. Kadanoff, I. Procaccia, and B. Shraiman, Phys. Rev. A **33**, 1141 (1986).
[27]L. P. Kadanoff, in *On Growth and Form, Fractal, and Nonfractal Patterns in Physics*, edited by H. E. Stanley and N. Ostrowky, NATO ASI Series E100 (Martinus Nijhoff, Dordrecht, 1986).
[28]P. Meakin, Phys. Rev. A (to be published).
[29]M. E. Cates and T. A. Witten, Phys. Rev. Lett. **56**, 2497 (1986).
[30]T. A. Witten, in *Physics of Finely Divided Matter*, edited by N. Boccara and M. Daccord (Springer, Berlin, 1985).
[31]P. Meakin, Phys. Lett. A **107**, 269 (1985).
[32]P. Meakin, J. Colloid Interface Sci. **102**, 505 (1984).
[33]J. G. Kirkwood and J. Riseman, J. Chem. Phys. **16**, 565 (1948).
[34]R. Zwanzig, J. Kiefer, and G. H. Weiss, Proc. Natl. Acad. Sci. U.S.A. **60**, 381 (1968).
[35]J. Rotne and S. Prager, J. Chem. Phys. **50**, 4831 (1969).
[36]H. Yamakawa, J. Chem. Phys. **53**, 436 (1970).
[37]J. A. McCammon and J. M. Deutch, Biopolymers **15**, 1397 (1976).
[38]T. A. Witten (private communication).
[39]Y. Kantor and T. A. Witten, J. Phys. Lett. (Paris) **45**, L675 (1984).